Probabilistic slope stability analysis by finite elements

D.V. Griffiths* and Gordon A. Fenton†

* Division of Engineering, Colorado School of Mines, U.S.A.
† Department of Engineering Mathematics, Dalhousie University, Canada

Abstract The paper investigates the probability of failure of a cohesive slope using both simple and more advanced probabilistic analysis tools. The influence of local averaging on the probability of failure of a test problem is thoroughly investigated. In the simple approach, classical slope stability analysis techniques are used, and the shear strength is treated as a single random variable. The advanced method, called the random finite element method (RFEM), uses elasto-plasticity combined with random field theory. The RFEM method is shown to offer many advantages over traditional probabilistic slope stability techniques, because it enables slope failure to develop naturally by "seeking out" the most critical mechanism. Of particular importance in this work, is the conclusion that simplified probabilistic analysis, in which spatial variability is ignored by assuming perfect correlation, can lead to unconservative estimates of the probability of failure. This contradicts the findings of other investigators using classical slope stability analysis tools.

1 Introduction

Slope stability analysis is a branch of geotechnical engineering that is highly amenable to probabilistic treatment, and has received considerable attention in the literature. The earliest papers appeared in the 1970s (e.g. Matsuo and Kuroda 1974, Alonso 1976, Tang *et al.* 1976, Vanmarcke 1977) and have continued steadily (e.g. D'Andrea and Sangrey 1982, Li and Lumb 1987, Mostyn and Li 1993, Chowdhury and Tang 1987, Whitman 1984, Wolff 1996, Lacasse (1994), Christian *et al.* 1994, Christian 1996, Lacasse and Nadim (1996), Hassan and Wolff 1999, Duncan 2000). Most recently, El-Ramly *et al.* 2002 produced a useful review of the literature on this topic, and also noted that the geotechnical profession was slow to adopt probabilistic approaches to geotechnical design, especially in traditional problems such as slopes and foundations.

Two main observations can be made in relation to the existing body of work on this subject. First, the vast majority of probabilistic slope stability analyses, while using novel and sometimes quite sophisticated probabilistic methodologies, continue to use classical slope stability analysis techniques (e.g. Bishop 1955) that have changed little in decades, and were never intended for use with highly variable soil shear strength distributions. An obvious deficiency of the traditional slope stability approaches, is that the shape of the failure surface (e.g. circular) is often fixed by the method, thus the failure mechanism is not allowed to "seek out" the most critical path through the soil. Second, while the importance of spatial correlation (or auto-correlation) and local averaging of statistical

geotechnical properties has long been recognized by some investigators (e.g. Mostyn and Soo 1990), it is still regularly omitted from many probabilistic slope stability analyses.

In recent years, the present authors have been pursuing a more rigorous method of probabilistic geotechnical analysis (e.g. Fenton and Griffiths 1993, Paice 1997, Griffiths and Fenton 2000), in which nonlinear finite element methods are combined with random field generation techniques. This method, called here the "Random Finite Element Method" (RFEM), fully accounts for spatial correlation and averaging, and is also a powerful slope stability analysis tool that does not require *a priori* assumptions relating to the shape or location of the failure mechanism.

In order to demonstrate the benefits of this method and to put it in context, this paper investigates the probabilistic stability characteristics of a cohesive slope using both the simple and more advanced methods. Initially, the slope is investigated using simple probabilistic concepts and classical slope stability techniques, followed by an investigation on the role of spatial correlation and local averaging. Finally, results are presented from a full-blown RFEM approach. Where possible throughout this paper, the Probability of Failure (p_f) is compared with the traditional Factor of Safety (FS) that would be obtained from charts or classical limit equilibrium methods.

The slope under consideration, known as the "Test Problem" is shown in Figure 1, and consists of undrained clay, with shear strength parameters $\phi_u = 0$ and c_u. In this study, the slope inclination and dimensions, given by β, H and D, and the saturated unit weight of the soil, γ_{sat} are held constant, while the undrained shear strength c_u is assumed to be a random variable. In the interests of generality, the undrained shear strength will be expressed in dimensionless form C, where $C = c_u/(\gamma_{sat}H)$.

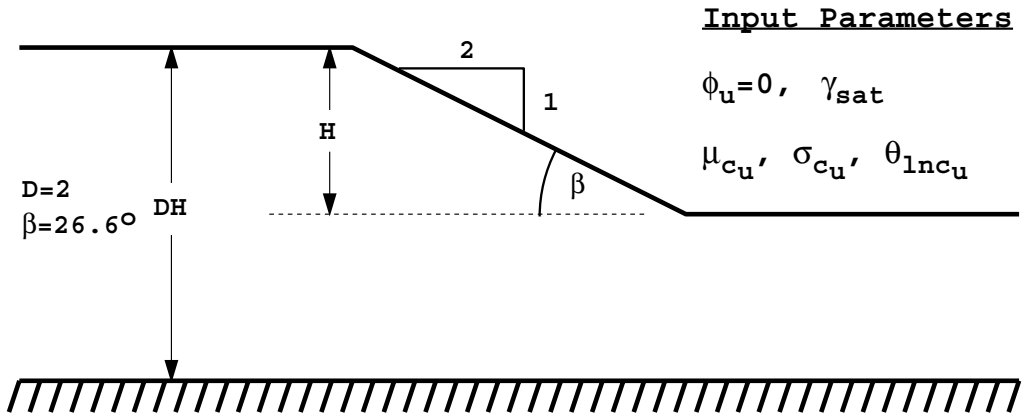

Figure 1. Cohesive slope test problem

2 Probabilistic description of shear strength

In this study, the shear strength C is assumed to be characterized statistically by a lognormal distribution defined by a mean, μ_C, and a standard deviation σ_C.

The probability density function of a lognormal distribution is given by,

$$f(C) = \frac{1}{C\ \sigma_{\ln C}\ \sqrt{2\pi}}\ \exp\left\{-\frac{1}{2}\left(\frac{\ln C - \mu_{\ln C}}{\sigma_{\ln C}}\right)^2\right\} \tag{1}$$

shown in Figure 2 for a typical case with $\mu_C = 100$ kN/m^2 and $\sigma_C = 50$ kN/m^2. The function encloses an area of unity, thus the probability of the strength dropping below a given value is easily found from standard tables. The mean and standard deviation can conveniently be expressed in terms of the dimensionless coefficient of variation defined as

$$V_C = \frac{\sigma_C}{\mu_C} \tag{2}$$

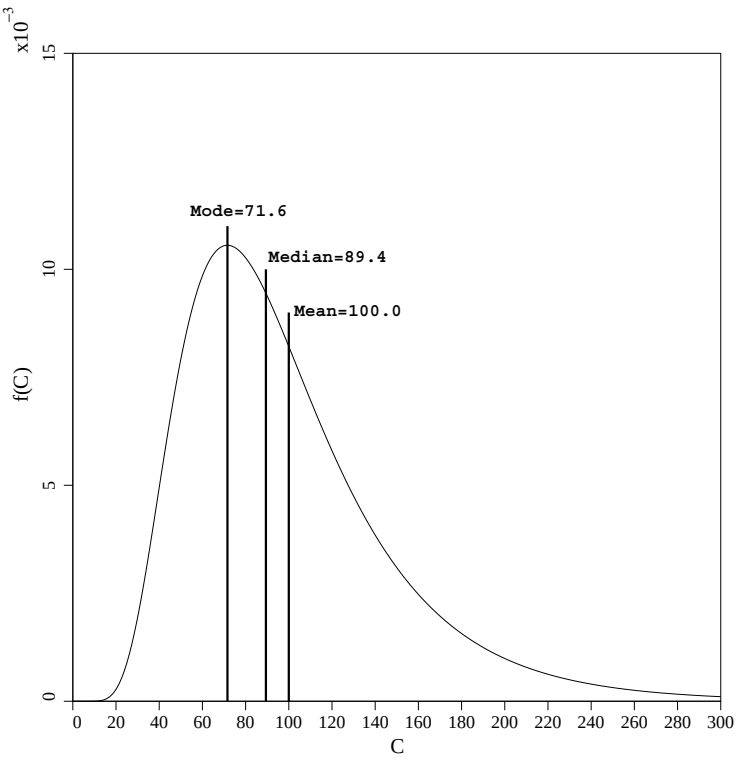

Figure 2. Typical log-normal distribution, with a mean of 100 and a standard deviation of 50 ($V_C = 0.5$)

Other useful relationships relating to the lognormal function include the standard deviation and mean of the underlying normal distribution as follows:

$$\sigma_{\ln C} = \sqrt{\ln\{1 + V_C^2\}} \tag{3}$$

$$\mu_{\ln C} = \ln \mu_C - \frac{1}{2}\sigma_{\ln C}^2 \tag{4}$$

Rearrangement of equations (3) and (4) gives the inverse relationships:

$$\mu_C = \exp\left(\mu_{\ln C} + \frac{1}{2}\sigma_{\ln C}^2\right) \tag{5}$$

$$\sigma_C = \mu_C\sqrt{\exp(\sigma_{\ln C}^2) - 1} \tag{6}$$

Finally the median and mode of a lognormal distribution are given by:

$$\text{Median}_C = \exp(\mu_{\ln C}) \tag{7}$$

$$\text{Mode}_C = \exp(\mu_{\ln C} - \sigma_{\ln C}^2) \tag{8}$$

A third parameter, the spatial correlation length $\theta_{\ln C}$ will also be considered in this study. Since the actual undrained shear strength field is lognormally distributed, its logarithm yields an "underlying" normal distributed (or Gaussian) field. The spatial correlation length is measured with respect to this underlying field, that is, with respect to $\ln C$. In particular, the spatial correlation length ($\theta_{\ln C}$) describes the distance over which the spatially random values will tend to be significantly correlated in the underlying Gaussian field. Thus, a large value of $\theta_{\ln C}$ will imply a smoothly varying field, while a small value will imply a ragged field. The spatial correlation length can be estimated from a set of shear strength data taken over some spatial region simply by performing the statistical analyses on the log-data. In practice, however, $\theta_{\ln C}$ is not much different in magnitude from the correlation length in real space and, for most purposes, θ_C and $\theta_{\ln C}$ are interchangeable given their inherent uncertainty in the first place. In the current study, the spatial correlation length has been non-dimensionalized by dividing it by the height of the embankment H and will be expressed in the form,

$$\Theta_C = \theta_{\ln C}/H \tag{9}$$

It has been suggested (see e.g. Lee *et al* 1983, Kulhawy *et al* 1991) that typical V_C values for undrained shear strength lie in the range 0.1-0.5. The spatial correlation length however, is less well documented and may well exhibit anisotropy, especially in the horizontal direction. While the advanced analysis tools used later in this study have the capability of modeling an anisotropic spatial correlation field, the spatial correlation, when considered, will be assumed to be isotropic.

3 Preliminary Deterministic Study

To put the probabilistic analyses in context, an initial deterministic study has been performed assuming a homogeneous soil. For the simple slope shown in Figure 1, the

Factor of Safety can readily be obtained from Taylor's (1937) charts or simple limit equilibrium methods to give Table 1.

Table 1. Factors of Safety Assuming Homogeneous Soil

C	FS
0.15	0.88
0.17	1.00
0.20	1.18
0.25	1.47
0.30	1.77

These results, shown plotted in Figure 3, indicate the linear relationship between C and FS. The figure also shows that the test slope becomes unstable when the shear strength parameter falls below $C = 0.17$.

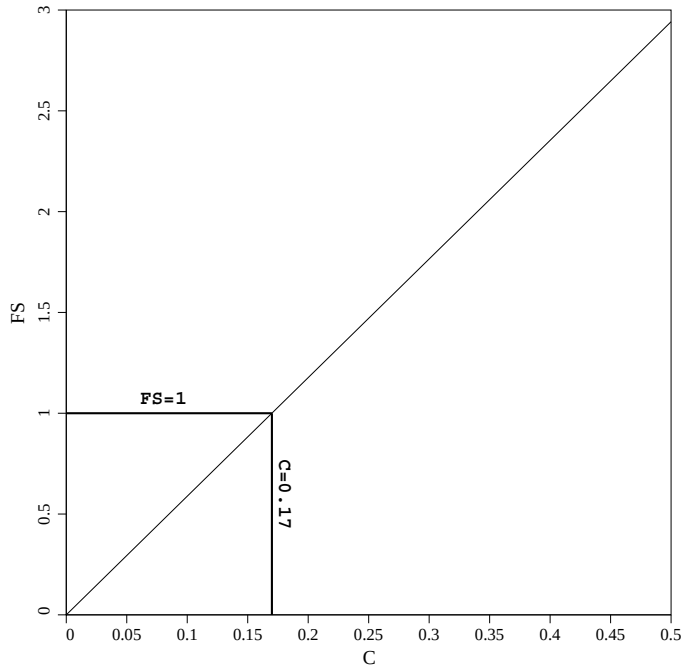

Figure 3. Linear relationship between FS and C for a cohesive slope with a slope angle of $\beta = 26.57^o$ and a depth ratio $D = 2$

4 Single random variable (SRV) approach

The first probabilistic analysis to be presented here investigates the influence of giving the shear strength C a lognormal probability density function similar to that shown in

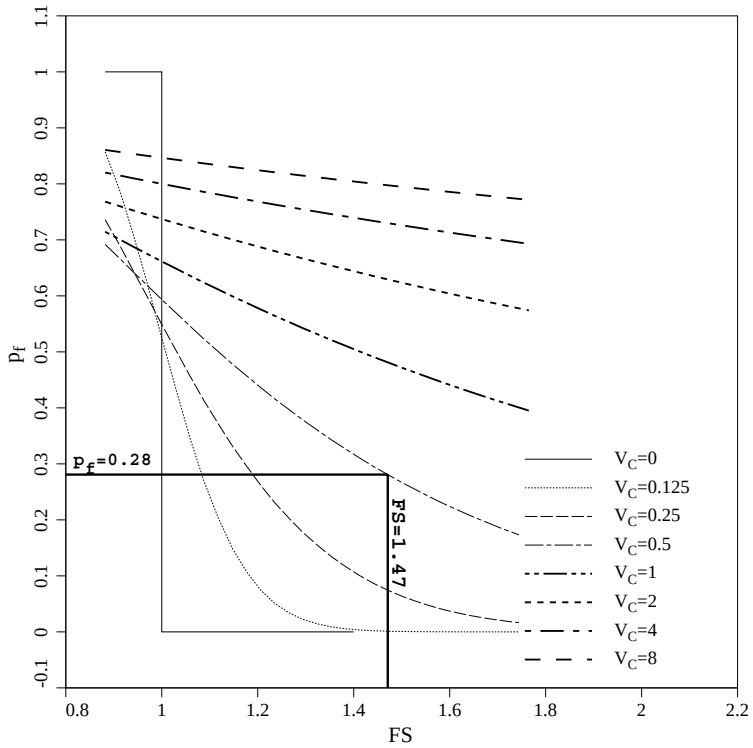

Figure 4. Probability of Failure vs. Factor of Safety (based on the mean) in a single random variable approach

Figure 2, based on a mean μ_C, and a standard deviation σ_C. The slope is assumed to have the same value of C everywhere, however the value of C is selected randomly from the lognormal distribution. Anticipating the random field analyses to be described later in this paper, this "single random variable approach" implies a spatial correlation length of $\Theta_C = \infty$, so no local averaging is applicable.

The Probability of Failure (p_f) in this case, is simply equal to the probability that the shear strength parameter C will be less than 0.17. Quantitatively, this equals the area of the probability density function corresponding to $C \leq 0.17$.

For example, if $\mu_C = 0.25$ and $\sigma_C = 0.125$ ($V_C = 0.5$), equations (3) and (4) give that the mean and standard deviation of the underlying normal distribution of the strength parameter are $\mu_{\ln C} = -1.498$ and $\sigma_{\ln C} = 0.472$.

The Probability of Failure is therefore given by:

$$p_f = p[C < 0.17] = \Phi\left(\frac{\ln 0.17 - \mu_{\ln C}}{\sigma_{\ln C}}\right) = 0.281 \tag{10}$$

where Φ is the cumulative standard normal distribution function.

This approach has been repeated for a range of μ_C and V_C values, for the slope under consideration, leading to Figure 4 which gives a direct relationship between the Factor of Safety and the Probability of Failure. It should be emphasized that the Factor of Safety in this plot is based on the value that would have been obtained if the slope had consisted of a homogeneous soil with a shear strength equal to the mean value μ_C from Figure 3.

From Figure 4, the Probability of Failure (p_f) clearly increases as the Factor of Safety decreases, however it is also shown that for $FS > 1$, the Probability of Failure increases as the V_C increases. The exception to this trend occurs when $FS < 1$. As shown in Figure 4, the Probability of Failure in such cases is understandably high, however the role of V_C is to have the opposite effect, with lower values of V_C tending to give the highest values of the probability of failure. This is explained by the "bunching up" of the shear strength distribution at low V_C rapidly excluding area to the right of the critical value of $C = 0.17$.

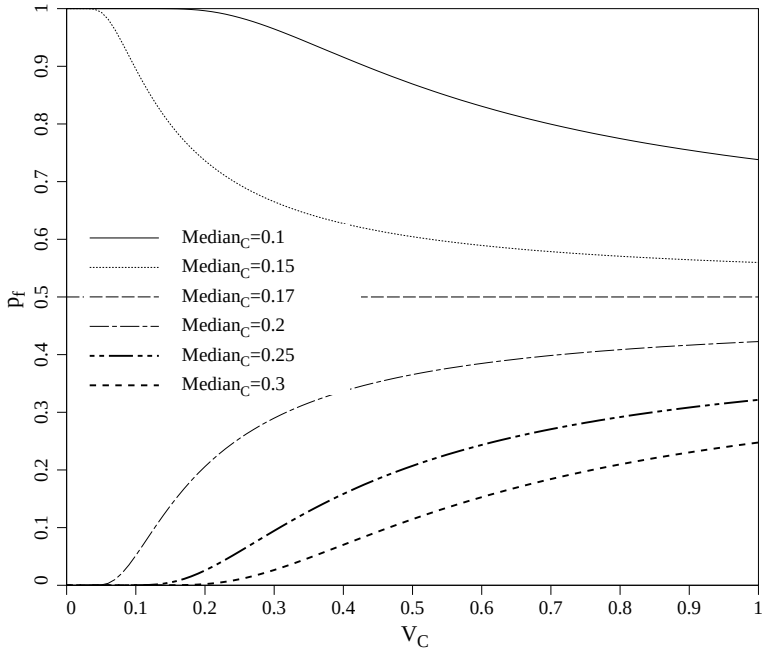

Figure 5. p_f vs. V_C for different Median$_C$ values

Figure 5 shows that the Median$_C$ is the key to understanding how the Probability of Failure changes in this analysis. When Median$_C < 0.17$, increasing V_C causes p_f to fall, whereas when Median$_C > 0.17$, increasing V_C causes p_f to rise.

While the single random variable approach described in this section leads to simple calculations, and useful qualitative comparisons between the Probability of Failure and the Factor of Safety, the quantitative value of the approach is more questionable. An important observation highlighted in Figure 4, is that a soil with a mean strength of $\mu_C = 0.25$ (implying $FS = 1.47$), would give a Probability of Failure as high as $p_f = 0.28$

for a soil with $V_C = 0.5$. Practical experience indicates that slopes with a Factor of Safety as high as $FS = 1.47$ rarely fail.

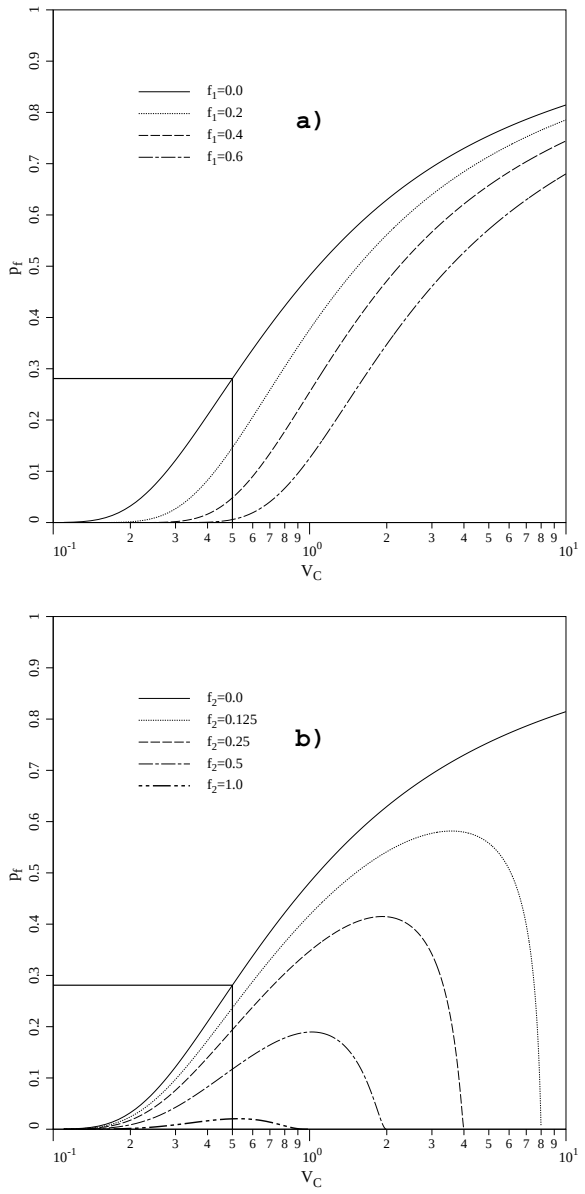

Figure 6. Influence of different mean strength factoring strategies on the Probability of Failure vs. Factor of Safety relationship. a) linear factoring b) standard deviation factoring. All curves assume FS=1.47 (based on $C_{des} = 0.25$)

An implication of this result is that either the perfectly correlated single random variable approach is entirely pessimistic in the prediction of the Probability of Failure, and/or it is unconservative to use the mean strength of a variable soil to estimate the Factor of Safety. Presented with a range of shear strengths at a given site, a geotechnical engineer would likely select a "pessimistic" or "lowest plausible" value for design, C_{des}, that would be lower than the mean. Assuming for the time being that the single random variable approach is reasonable, Figure 6 shows the influence on the Probability of Failure of two strategies for factoring the mean strength μ_C prior to calculating the Factor of Safety for the test problem.

In Figure 6a, a linear reduction in the mean strength has been proposed using a factor f_1, where:

$$C_{des} = \mu_C(1 - f_1) \tag{11}$$

and in Figure 6b, the mean strength has been reduced by a factor f_2 of the standard deviation, where:

$$C_{des} = \mu_C - f_2\sigma_C \tag{12}$$

All the results shown in Figure 6 assume that after factorization, $C_{des} = 0.25$, implying a Factor of Safety $FS = 1.47$. The Probability of Failure of $p_f = 0.28$ with no factorization $f_1 = f_2 = 0$, has also been highlighted for the case of $V_C = 0.5$. In both cases, an increase in the strength reduction factor reduces the Probability of Failure, which is to be expected, however the nature of the two sets of reduction curves is quite different, especially for higher values of V_C. From the linear mean strength reduction (equation 11), $f_1 = 0.6$ would result in a Probability of Failure of about 0.6%. By comparison, a mean strength reduction of one standard deviation given by $f_2 = 1$ (equation 12), would result in a Probability of Failure of about 2%. Figure 6a shows a gradual reduction of the Probability of Failure for all values of f_1 and V_C, however a quite different behavior is shown in Figure 6b, where standard deviation factoring results in a very rapid reduction in the Probability of Failure, especially for higher values of $V_C > 2$. This curious result is easily explained by the functional relationship between p_f and V_C, where the design strength can be written as:

$$C_{des} = 0.25 = \mu_C - f_2\sigma_C = \mu_C(1 - f_2V_C) \tag{13}$$

hence as $V_C \to 1/f_2$, $\mu_C \to \infty$. With the mean strength so much greater than the critical value of 0.17, the Probability of Failure falls very rapidly towards zero.

5 Spatial Correlation

Implicit in the single random variable approach described above, is that the spatial correlation length is infinite. In other words only homogeneous slopes are considered, in which the property assigned to the slope is taken at random from a lognormal distribution. A more realistic model would properly take account of smaller spatial correlation lengths in which the soil strength is allowed to vary spatially within the slope. The parameter that controls this is the spatial correlation length $\theta_{\ln C}$ as discussed previously. In this work, an exponentially decaying (Markovian) correlation function is used of the form:

$$\rho = e^{-\frac{2\tau}{\theta_{\ln C}}} \tag{14}$$

where ρ is the familiar correlation coefficient, and τ is the absolute distance between two points in the random field. A plot of this function is given in Figure 7 and indicates, for example, that the strength at two points separated by $\theta_{\ln C}$ ($\tau/\theta_{\ln C} = 1$) will have an expected correlation of $\rho = 0.135$. This correlation function is merely a way of representing the field observation that soil samples taken close together are more likely to have similar properties, than samples taken from far apart. There is also the issue of anisotropic spatial correlation, in that soil is likely to have longer spatial correlation lengths in the horizontal direction than in the vertical, due to the depositional history. While the tools described in this paper can take account of anisotropy, this refinement is left for future studies.

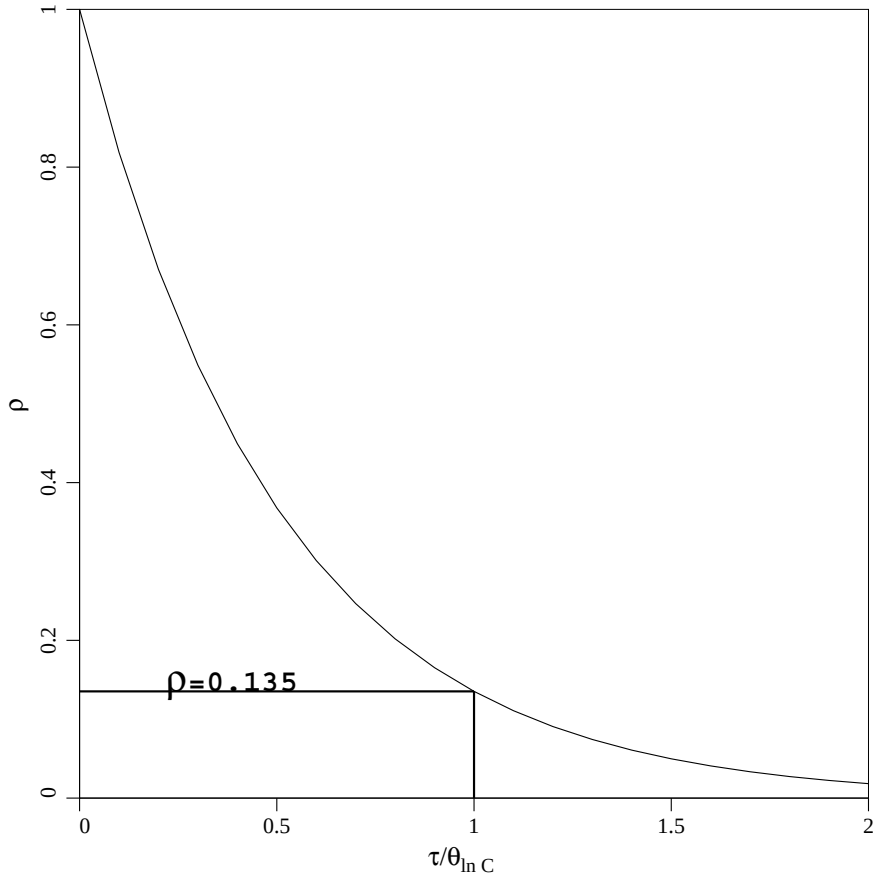

Figure 7. Markov correlation function

6 The Random Finite Element Method (RFEM)

A powerful and general method of accounting for spatially random shear strength parameters and spatial correlation, is the Random Finite Element Method (RFEM) which combines elasto-plastic finite element analysis with random field theory generated using the Local Average Subdivision Method (Fenton and Vanmarcke 1990). The methodology has been described in detail in other publications (e.g. Griffiths and Fenton 2001), so only a brief description will be repeated here.

A typical finite element mesh for the test problem considered in this paper is shown in Figure 8. The majority of the elements are square, however the elements adjacent to the slope are degenerated into triangles.

The code developed by the authors enables a random field of shear strength values to be generated and mapped onto the finite element mesh, taking full account of element size in the local averaging process. In a random field, the value assigned to each cell (or finite element in this case) is itself a random variable, thus the mesh of Figure 8, which has 910 finite elements, contains 910 random variables.

The random variables can be correlated to one another by controlling the spatial correlation length $\theta_{\ln C}$ as described previously, hence the single random variable approach discussed in the previous section where the spatial correlation length is implicitly set to infinity, can now be viewed as a special case of a much more powerful analytical tool. Figures 9a and b show typical meshes corresponding to different spatial correlation lengths. Figure 9a shows a relatively low spatial correlation length of $\Theta_C = 0.2$ and Figure 9b shows a relatively high spatial correlation length of $\Theta_C = 2$. Dark and light regions depict "weak" and "strong" soil respectively. It should be emphasized that both these shear strength distributions come from the same lognormal distribution, and it is only the spatial correlation length that is different.

In brief, the analyses involve the application of gravity loading, and the monitoring of stresses at all the Gauss points. The slope stability analyses use an elastic-perfectly plastic stress-strain law with a Tresca failure criterion which is appropriate for "undrained clays". If the Tresca criterion is violated, the program attempts to redistribute excess stresses to neighboring elements that still have reserves of strength. This is an iterative process which continues until the Tresca criterion and global equilibrium are satisfied at all points within the mesh under quite strict tolerances.

Plastic stress redistribution is accomplished using a viscoplastic algorithm with 8-node quadrilateral elements and reduced integration in both the stiffness and stress redistribution parts of the algorithm. The theoretical basis of the method is described more fully in Chapter 6 of the text by Smith and Griffiths (1998), and for a detailed discussion of the method applied to slope stability analysis, the reader is referred to Griffiths and Lane (1999).

For a given set of input shear strength parameters (mean, standard deviation and spatial correlation length), Monte-Carlo simulations are performed. This means that the slope stability analysis is repeated many times until the statistics of the output quantities of interest become stable. Each "realization" of the Monte-Carlo process differs in the locations at which the strong and weak zones are situated. For example, in one realization, weak soil may be situated in the locations where a critical failure

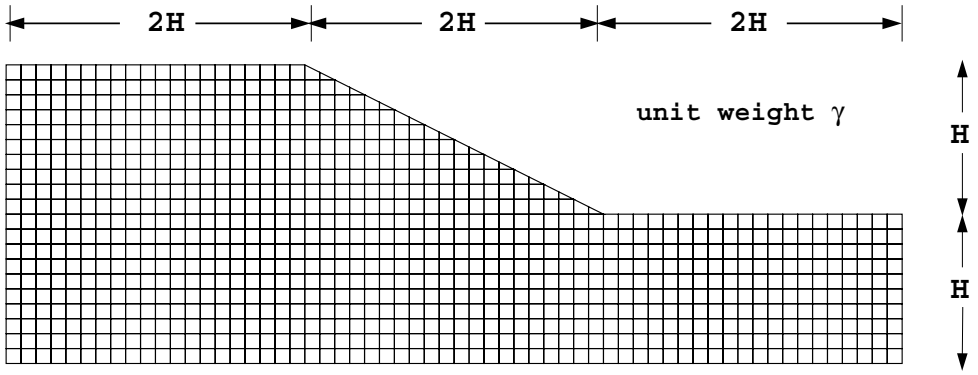

Figure 8. Mesh used for RFEM slope stability analyses

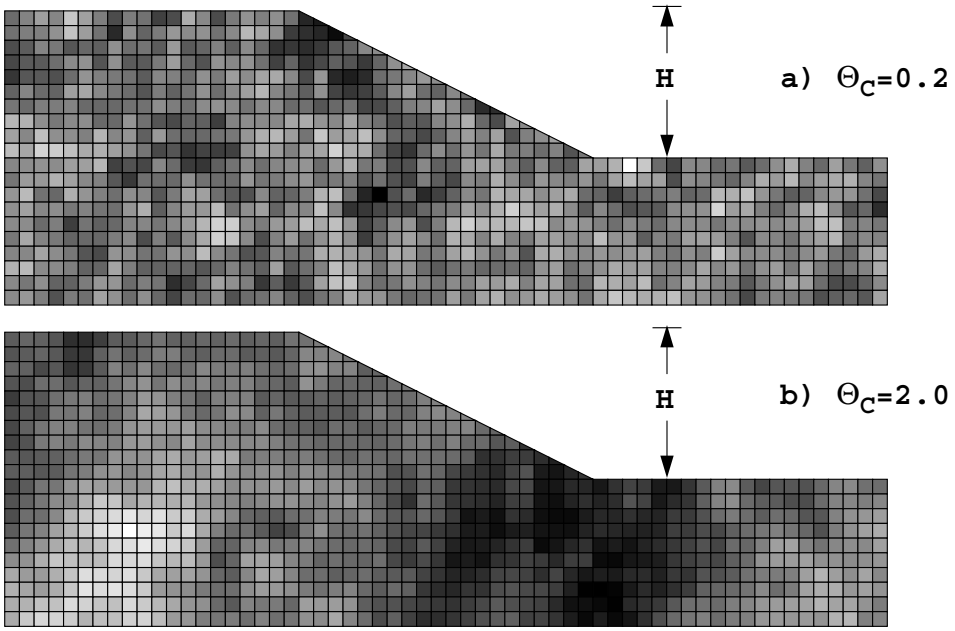

Figure 9. Influence of the scale of fluctuation in RFEM analysis

mechanism develops causing the slope to fail, whereas in another, strong soil in those locations means that the slope remains stable.

In this study, it was determined that 1000 realizations of the Monte-Carlo process for each parametric group, was sufficient to give reliable and reproducible estimates of the Probability of Failure, which was simply defined as the proportion of the 1000 Monte-Carlo slope stability analyses that failed.

In this study,"failure" was said to have occurred if, for any given realization, the algorithm was unable to converge within 500 iterations. While the choice of 500 as the iteration ceiling is subjective, Figure 10 confirms, for the case of $\mu_C = 0.25$ and $\Theta_C = 1$, that the Probability of Failure defined this way, is stable for iteration ceilings greater than about 200.

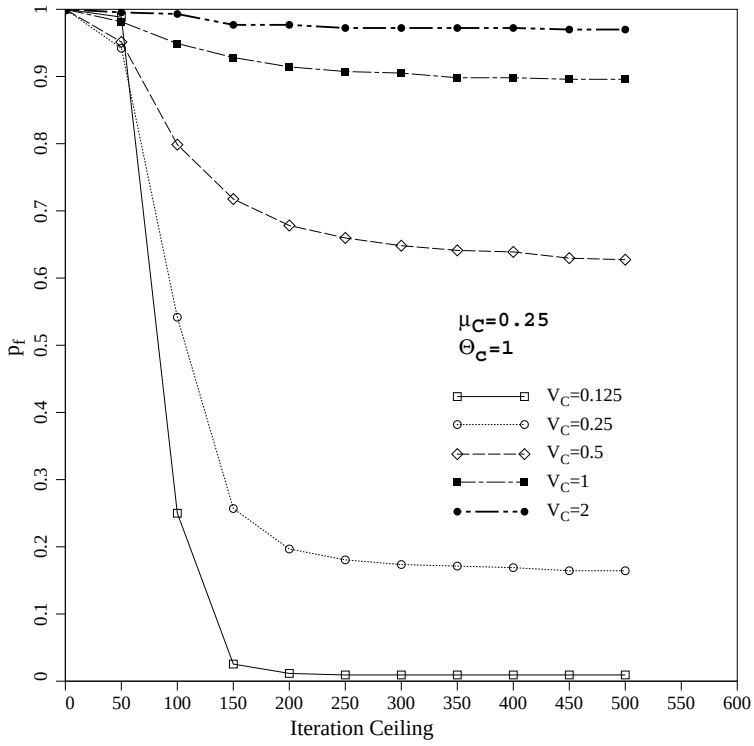

Figure 10. Influence the plastic iteration ceiling on the computed Probability of Failure

7 Local Averaging

The input parameters relating to the mean, standard deviation and spatial correlation length of the undrained strength, are assumed to be defined at the point level. While statistics at this resolution are obviously impossible to measure in practice, they represent a fundamental baseline of the inherent soil variability which can be corrected through local averaging to take account of the sample size.

In the context of the RFEM approach, each element is assigned a constant property at each realization of the Monte-Carlo process. The "sample" is represented by the size of each finite elements used to discretize the slope. If the point distribution is normal, local averaging results in a reduced variance but the mean is unaffected. In a lognormal

distribution however, both the mean and the standard deviation are reduced by local averaging. This is because from equations (5) and (6), the mean of a lognormal relationship depends on both the mean *and* the variance of the underlying normal log-relationship. Thus the cruder the discretization of the slope stability problem and the larger the elements, the greater the influence of local averaging in the form of a reduced mean and standard deviation. These adjustments to the point statistics are fully accounted for in the RFEM, and are implemented before the elasto-plastic finite element slope stability analysis takes place.

8 Variance reduction over a square finite element

In this section, the algorithm used to compute the locally averaged statistics applied to the mesh is described.

A lognormal distribution of a random variable C, with point statistics given by a mean μ_C, a standard deviation σ_C and spatial correlation length $\theta_{\ln C}$, is to be mapped onto a mesh of square finite elements. Each element will be assigned a single value of the undrained strength parameter.

The locally averaged statistics over the elements will be referred to here as the "area" statistics with the subscript A. Thus, with reference to the underlying normal distribution of $\ln C$, the mean, which is unaffected by local averaging, is given by $\mu_{\ln C_A}$, and the standard deviation, which is affected by local averaging is given by $\sigma_{\ln C_A}$.

The variance reduction factor due to local averaging γ, is defined:

$$\gamma = \left(\frac{\sigma_{\ln C_A}}{\sigma_{\ln C}} \right)^2 \tag{15}$$

and is a function of the element size and the correlation function from equation (14), repeated here in the form,

$$\rho = \exp\left\{ -\frac{2}{\theta_{\ln C}} \sqrt{\tau_x^2 + \tau_y^2} \right\} \tag{16}$$

where τ_x is the difference between the $x-$coordinates of any two points in the random field, and τ_y is the difference between the y-coordinates.

For a square finite element of side length $\alpha\theta_{\ln C}$ as shown in Figure 11, it can be shown (Vanmarcke 1984) that for an isotropic spatial correlation field, the variance reduction factor is given by:

$$\gamma = \frac{4}{(\alpha\theta_{\ln C})^4} \int_0^{\alpha\theta_{\ln C}} \int_0^{\alpha\theta_{\ln C}} \exp\left\{ -\frac{2}{\theta_{\ln C}} \sqrt{x^2 + y^2} \right\} (\alpha\theta_{\ln C} - x)(\alpha\theta_{\ln C} - y)\, dx\, dy \tag{17}$$

Numerical integration of this function leads to the variance reduction values given in Table 2, and shown plotted in Figure 11.

Table 2. Variance reduction over a square element

α	γ
0.01	0.9896
0.1	0.9021
1	0.3965
10	0.0138

The figure indicates that elements that are small relative to the correlation length ($\alpha \to 0$) lead to very little variance reduction ($\gamma \to 1$), whereas elements that are large relative to the correlation length can lead to very significant variance reduction ($\gamma \to 0$).

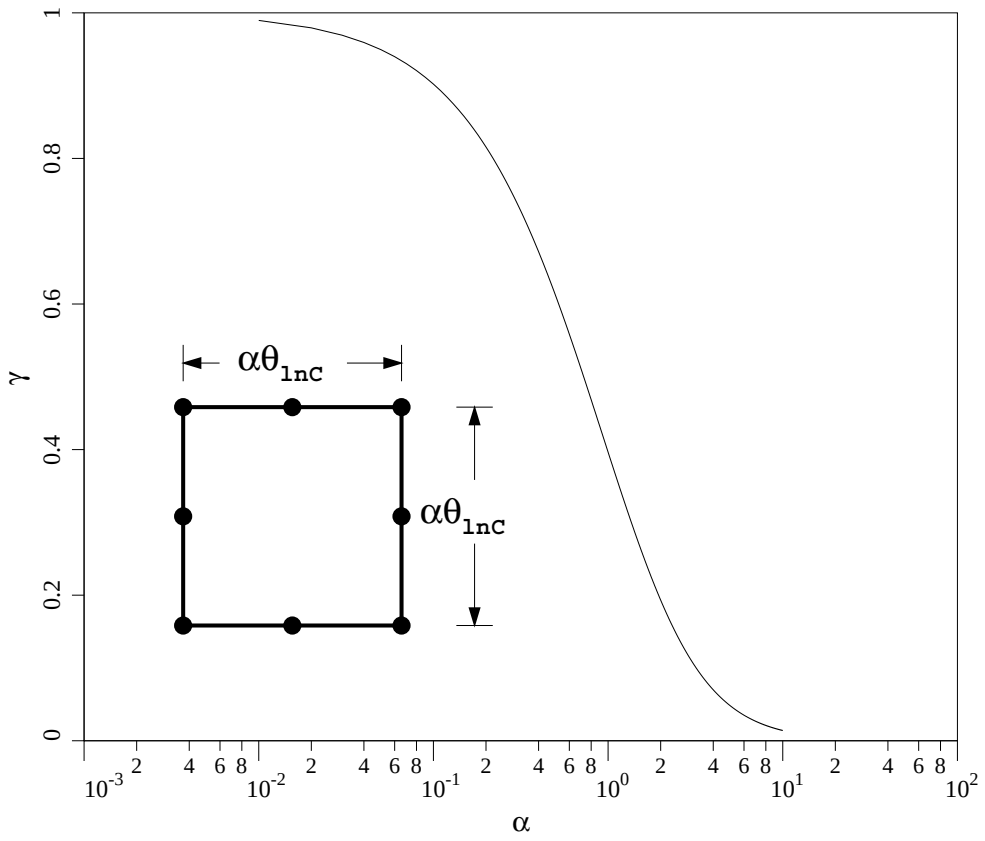

Figure 11. Variance reduction function over a square element of side length $\alpha\theta_{\ln C}$ with a Markov correlation function

The statistics of the underlying log-field, including local averaging, are therefore given by:

$$\sigma_{\ln C_A} = \sigma_{\ln C}\sqrt{\gamma} \tag{18}$$

and

$$\mu_{\ln C_A} = \mu_{\ln C} \tag{19}$$

which leads to the following statistics of the lognormal field, including local averaging, that is actually mapped onto the finite element mesh from equations (5) and (6), thus

$$\mu_{C_A} = \exp\left(\mu_{\ln C_A} + \frac{1}{2}\sigma^2_{\ln C_A}\right) \tag{20}$$

$$\sigma_{C_A} = \mu_{C_A}\sqrt{\exp(\sigma^2_{\ln C_A}) - 1} \tag{21}$$

It is instructive to consider the range of locally averaged statistics, since this helps to explain the influence of the spatial correlation length $\Theta_C (= \theta_{\ln C}/H)$ on the Probability of Failure in the RFEM slope analyses described in the next section.

Expressing the mean and the coefficient of variation of the locally averaged variable as a proportion of the point values of these quantities, leads to Figures 12a and 12b respectively. In both cases, there is virtually no reduction due to local averaging for elements that are small relative to the spatial correlation length ($\alpha \to 0$). This is to be expected, since the elements are able to model the point field quite accurately. For larger elements relative to the spatial correlation length however, Figure 12a indicates that the average of the locally averaged field tends to a constant equal to the median, and Figure 12b indicates that the coefficient of variation of the locally averaged field tends to zero.

From equations (18) to (21), the expression plotted in Figure 12a for the mean can be written as,

$$\frac{\mu_{C_A}}{\mu_C} = \frac{1}{(1+V_C^2)^{(1-\gamma)/2}} \tag{22}$$

which gives that when $\gamma \to 0$, $\mu_{C_A}/\mu_C \to 1/(1+V_C^2)^{1/2}$, thus $\mu_{C_A} \to e^{\mu_{\ln C}} = \text{Median}_C$.

The expression plotted in Figure 12b for the coefficient of variation of the locally averaged variable can be written as,

$$\frac{V_{C_A}}{V_C} = \frac{\sqrt{(1+V_C^2)^{\gamma} - 1}}{V_C} \tag{23}$$

which gives that when $\gamma \to 0$, $V_{C_A}/V_C \to 0$, thus $V_{C_A} \to 0$.

Further examination of equations (22) and (23) shows that for all values of γ,

$$\text{Median}_{C_A} = \text{Median}_C \tag{24}$$

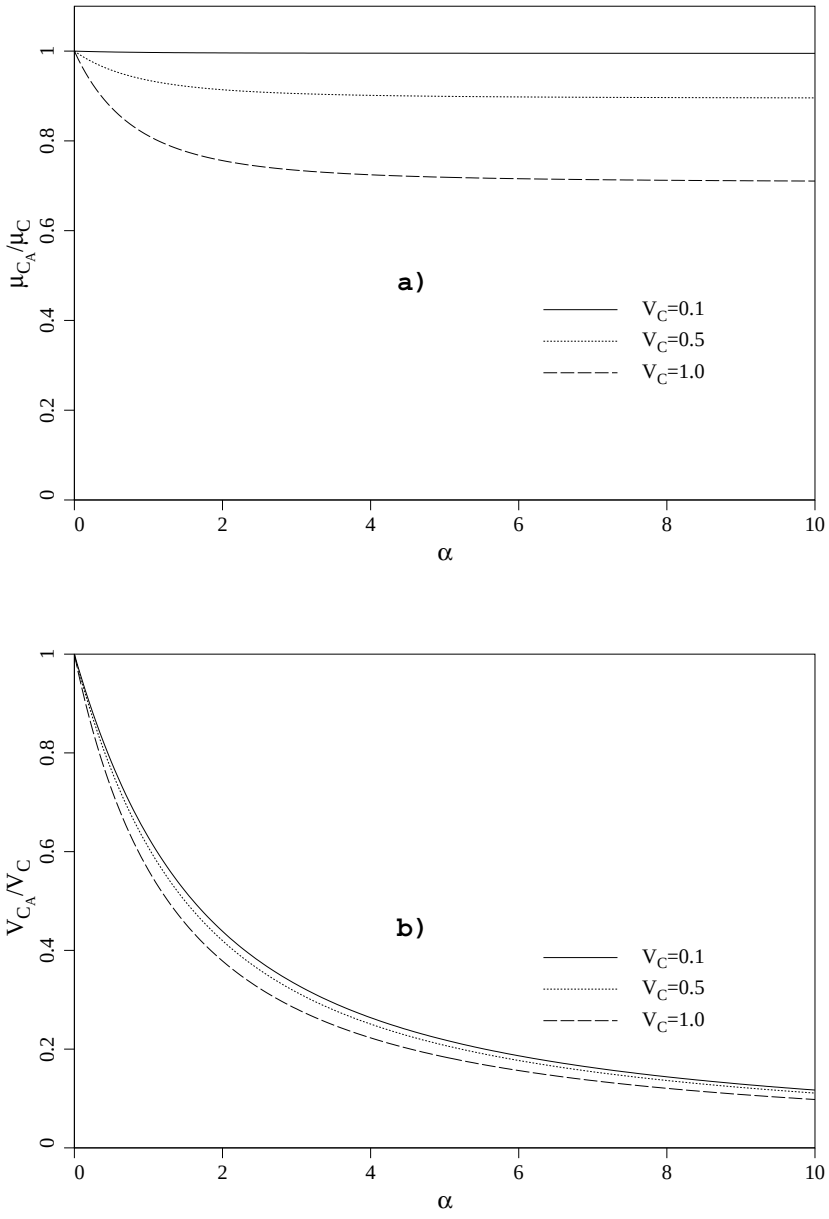

Figure 12. Influence of element size expressed in the form of a size parameter α on local averaging. a) Influence on the mean, and b) Influence on the coefficient of variation

In Summary,

1. local averaging reduces both the mean and the variance of a lognormal point distribution.

2. local averaging preserves the Median of the point distribution, and

3. in the limit, local averaging removes all variance, and the mean tends to the Median.

9 Locally averaged single random variable approach

In this section the Probability of Failure is reworked with the single random variable approach using properties derived from local averaging over an individual finite element, termed "finite element locally averaged properties" throughout the rest of this paper. With reference to the mesh shown in Figure 8, the square elements have a side length of $0.1H$, thus $\Theta_C = 0.1/\alpha$. Figure 13 shows the probability of failure p_f as a function of Θ_C for a range of input point coefficients of variation, with the point mean fixed at $\mu_C = 0.25$. The Probability of Failure is defined, as before, by $p[C < 0.17]$, but this time the calculation is based on the finite element locally averaged properties, μ_{C_A} and σ_{C_A} from equations 20 and 21. The figure clearly shows two tails to the results, with $p_f \to 1$ as $\Theta_C \to 0$ for all $V_C > 1.0783$, and $p_f \to 0$ as $\Theta_C \to 0$ for all $V_C < 1.0783$. The horizontal line at $p_f = 0.5$ is given by $V_C = 1.0783$, which is the special value of the coefficient of variation that causes the $\text{Median}_C = 0.17$.

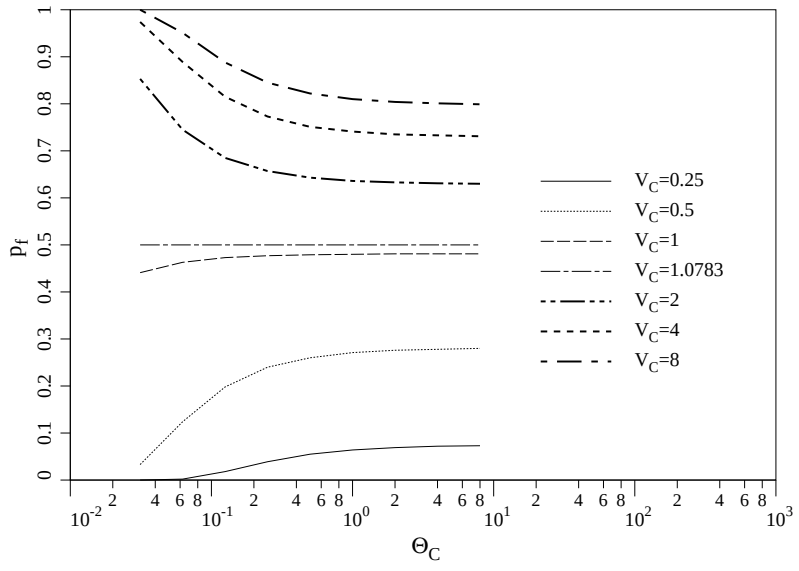

Figure 13. Probability of Failure vs. Spatial Correlation Length based on finite element locally averaged properties. The mean is fixed at $\mu_C = 0.25$

Recalling Table 1, this is the critical value of C that would give $FS = 1$ in the test slope. Higher values of V_C lead to $\text{Median}_C < 0.17$ and a tendency for $p_f \to 1$ as $\Theta_C \to 0$. Conversely, lower values of V_C lead to $\text{Median}_C > 0.17$ and a tendency for $p_f \to 0$. Figure 14 shows the same data plotted the other way round with V_C along the abscissa. This figure clearly shows the full influence of spatial correlation in the range $0 \leq \Theta_C < \infty$. All the curves cross over at the critical value of $V_C = 1.0783$, and it is of interest to note the step function corresponding to $\Theta_C = 0$ when p_f changes suddenly from zero to unity.

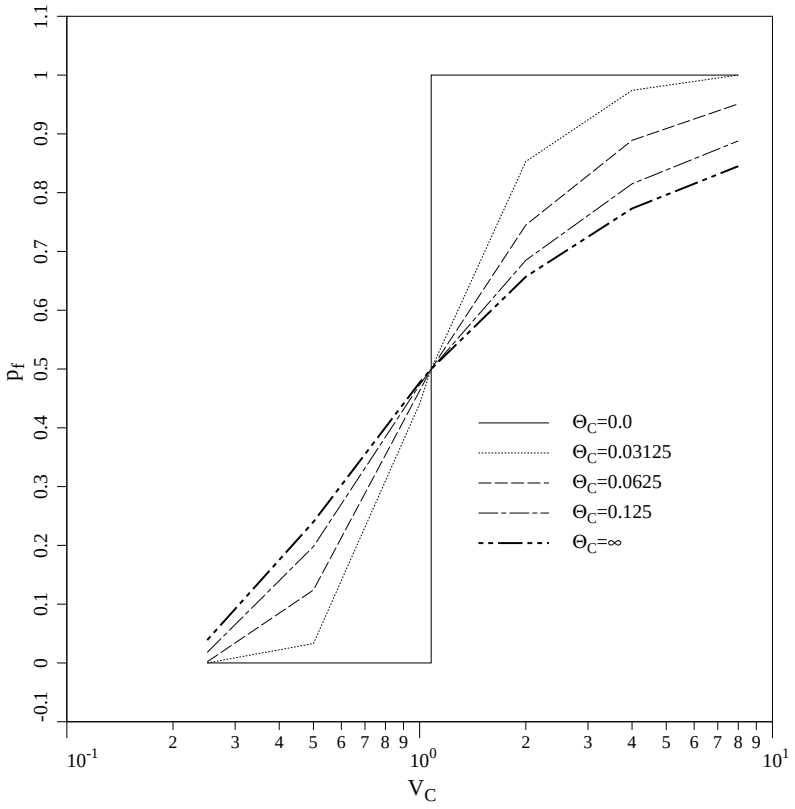

Figure 14. Probability of Failure vs. Coefficient of Variation based on finite element locally averaged properties. The mean is fixed at $\mu_C = 0.25$

It should be emphasized that the results presented in this section involved no finite element analysis, and were based solely on an SRV approach with statistical properties based on finite element locally averaged properties based on a typical finite element of the mesh in Figure 8.

10 Results of RFEM Analyses

In this section, the results of full nonlinear RFEM analyses with Monte-Carlo simulations are described, based on a range of parametric variations of μ_C, V_C and Θ_C.

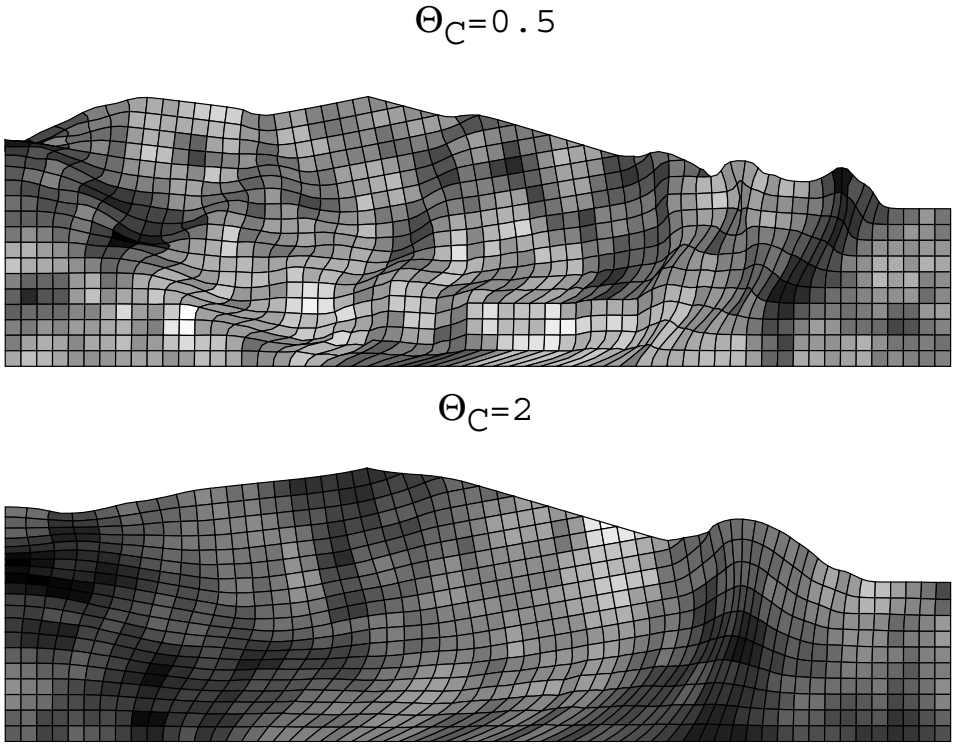

Figure 15. Typical random field realizations and deformed mesh at slope failure for two different spatial correlation lengths

In the elasto-plastic RFEM approach, the failure mechanism is free to "seek out" the weakest path through the soil. Figure 15 shows two typical random field realizations and the associated failure mechanisms for slopes with $\Theta_C = 0.5$ and $\Theta_C = 2$. The convoluted nature of the failure mechanisms, especially when $\Theta_C = 0.5$, would defy analysis by conventional slope stability analysis tools. While the mechanism is attracted to the weaker zones within the slope, it will inevitably pass through elements assigned many different strength values. This weakest path determination, and the strength averaging that goes with it, occurs quite naturally in the finite element slope stability method, and represents a very significant improvement over traditional limit equilibrium approaches to probabilistic slope stability, in which local averaging, if included at all, has to be computed over a failure mechanism that is pre-set the particular analysis method (e.g. a circular failure mechanism when using Bishop's Method).

Fixing the point mean strength at $\mu_C = 0.25$, Figures 16 and 17 show the effect of the spatial correlation length Θ_C and the coefficient of variation V_C on the probability of failure for the test problem. Figure 16 clearly indicates two branches, with the Probability of Failure tending to unity or zero for higher and lower values of V_C, respectively. This behavior is qualitatively similar to that observed in Figure 13, in which a single random variable approach was used to predict the Probability of Failure based solely on finite element locally averaged properties.

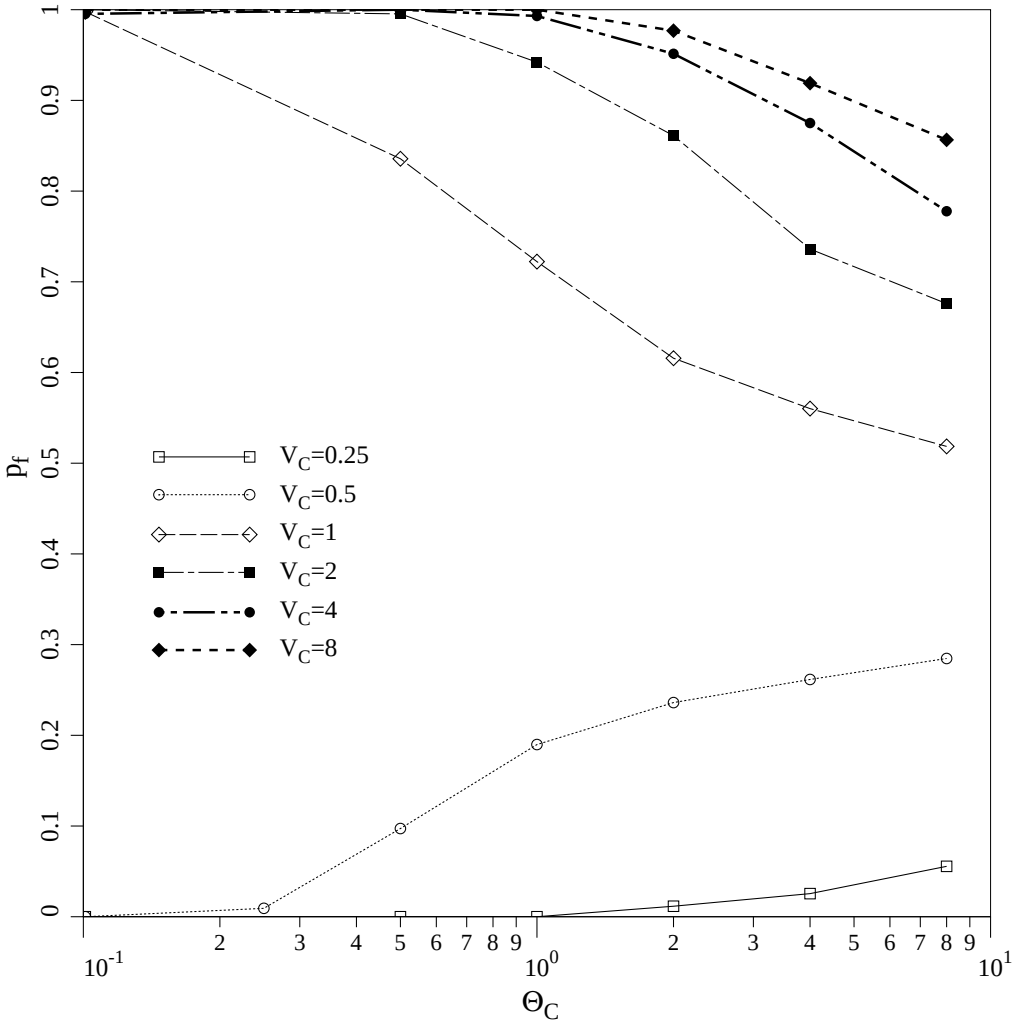

Figure 16. Probability of Failure vs. Spatial Correlation Length from RFEM. The mean is fixed at $\mu_C = 0.25$

Figure 17 shows the same results as Figure 16, but plotted the other way round with the coefficient of variation along the abscissa. Figure 17 also shows the theoretically obtained result corresponding to $\Theta_C = \infty$, indicating that a single random variable approach with no local averaging will overestimate the Probability of Failure (conservative) when the coefficient of variation is relatively small and underestimate the Probability of Failure (unconservative) when the coefficient of variation is relatively high. Figure 17 also confirms that the single random variable approach described earlier in the paper, which gave $p_f = 0.28$ corresponding to $\mu_C = 0.25$ and $V_C = 0.5$ with no local averaging, is indeed pessimistic. The RFEM results show that the inclusion of spatial correlation and local averaging in this case will always lead to a smaller Probability of Failure.

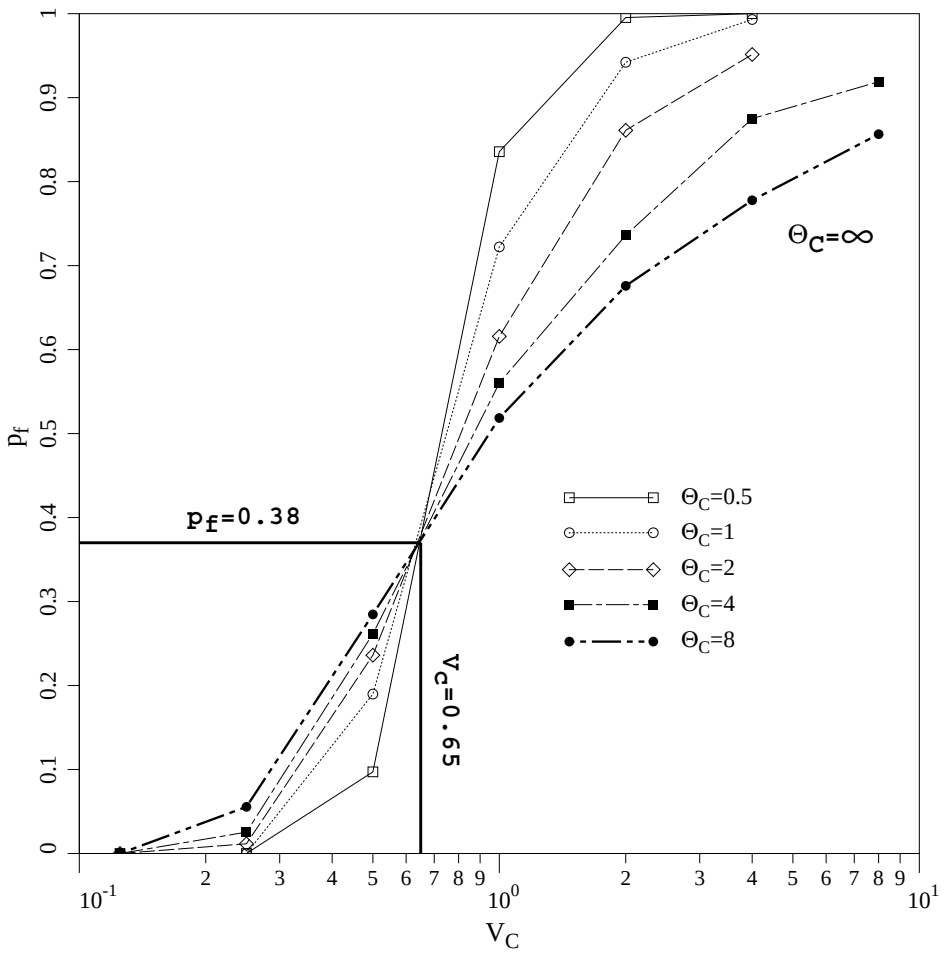

Figure 17. Probability of Failure vs. Coefficient of Variation from RFEM. The mean is fixed at $\mu_C = 0.25$

Comparison of Figures 13 and 14, with Figures 16 and 17, highlights the influence of the finite element approach to slope stability, where the failure mechanism is free to locate itself optimally within the mesh. From Figures 14 and 17, it is clear that the "weakest path" concept made possible by the RFEM approach has resulted in the crossover point falling to lower values of both V_C and p_f. With only finite element local averaging, the crossover occurred at $V_C = 1.0783$, whereas by the RFEM it occurred at $V_C \approx 0.65$. In terms of the Probability of Failure with only finite element local averaging, the crossover occurred at $p_f = 0.5$ whereas by the RFEM it occurred at $p_f \approx 0.38$. The RFEM solutions show that the single random variable approach becomes unconservative over a wider range of V_C values than would be indicated by finite element local averaging alone.

Figure 18 gives a direct comparison between Figures 13 and 16, indicating clearly that for higher values of V_C, RFEM always gives a higher probability of Failure than when using finite element local averaging alone. This is caused by the weaker elements in the distribution dominating the strength of the slope and the failure mechanism "seeking out" the weakest path through the soil.

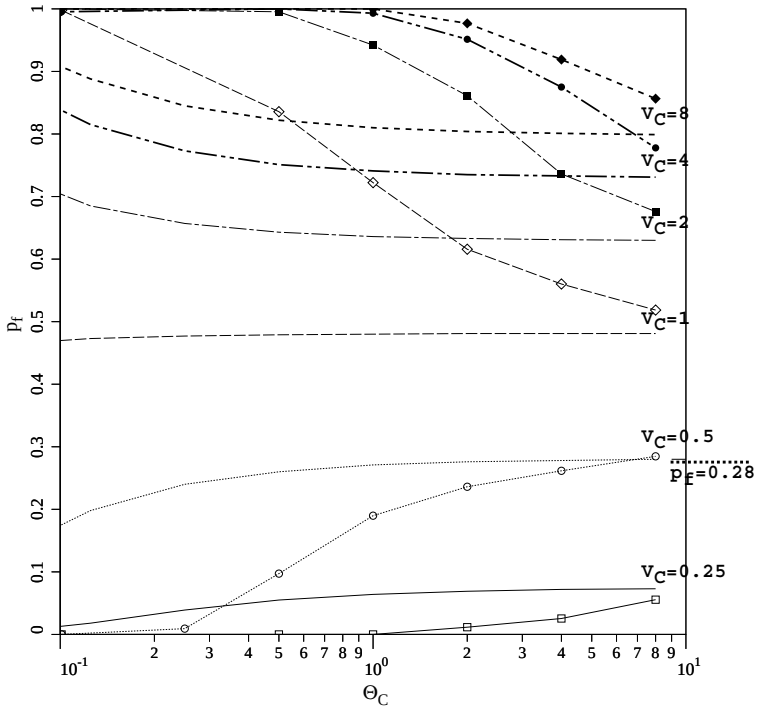

Figure 18. Comparison of the Probability of Failure predicted by RFEM and by finite element local averaging only. The curve with plotted points comes from the RFEM analyses.The mean is fixed at $\mu_C = 0.25$

At lower values of V_C, the locally averaged results tends to overestimate the Probability of Failure and give conservative results compared with RFEM. In this case the stronger elements of the slope are dominating the solution and the higher median combined with the "bunching up" of the locally averaged solution at low values of Θ_C, means that potential failure mechanisms cannot readily find a weak path through the soil.

In all cases, as Θ_C increases, the RFEM and the locally averaged solutions converge on the single random variable solution corresponding to $\Theta_C = \infty$ with no local averaging. The $p_f = 0.28$ value, corresponding to $V_C = 0.5$, and discussed earlier in the paper is also indicated on Figure 18.

All of the above results and discussion in this section so far were applied to the test slope from Figure 1 with the mean strength fixed at $\mu_C = 0.25$ corresponding to a Factor of Safety (based on the mean) of 1.47. In the next set of results μ_C is varied while V_C is held constant at 0.5. Figure 19 shows the relationship between FS (based on the mean) and p_f assuming finite element local averaging only, and Figure 20 shows the same relationship as computed using RFEM.

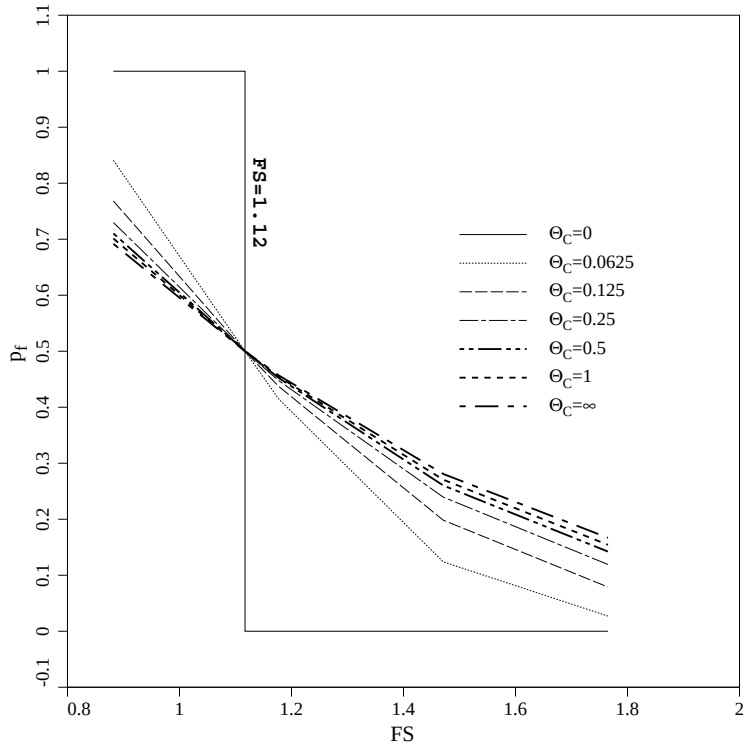

Figure 19. Probability of Failure vs. Factor of Safety (based on the mean) using finite element local averaging only for the test slope. The coefficient of variation is fixed at $V_C = 0.5$

Figure 19, based on finite element local averaging only, shows the full range of behavior for $0 \leq \Theta_C < \infty$. The figure shows that Θ_C only starts to have a significant influence on the FS vs. p_f relationship when the correlation length becomes significantly smaller than the slope height ($\Theta_C << 1$). The step function in which p_f jumps from zero to unity, occurs when $\Theta_C = 0$ and corresponds to a local average having zero variance. In this limiting case, the local average of the soil is deterministic, yielding a constant strength everywhere in the slope. With $V_C = 0.5$, the critical value of mean shear strength that would give $\mu_{C_A} = \text{Median}_C = 0.17$ is easily shown by equation 22 to be $\mu_C = 0.19$, which corresponds to a $FS = 1.12$. For higher values of Θ_C, the relationship between FS and p_f is quite "bunched up", and generally insensitive to Θ_C. For example, there is little difference between the curves corresponding to $\Theta_C = \infty$ and $\Theta_C = 0.5$. It should also be observed from Figure 19, that for $FS > 1.12$, failure to account for local averaging by assuming $\Theta_C = \infty$ is conservative, in that the predicted p_f is higher than it should be. When $FS < 1.12$ however, failure to account for local averaging is unconservative.

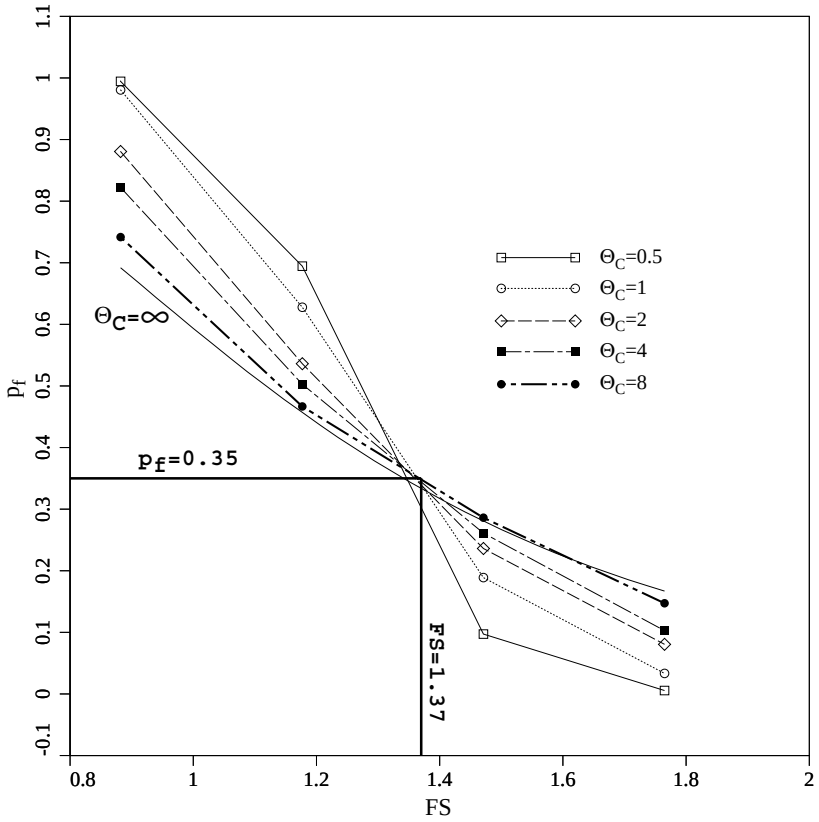

Figure 20. Probability of Failure vs. Factor of Safety (based on the mean) using RFEM for the test slope. The coefficient of variation is fixed at $V_C = 0.5$

Figure 20 gives the same relationships as computed using RFEM. By comparison with Figure 19, the RFEM results are more spread out, implying that the Probability of Failure is more sensitive to the spatial correlation length Θ_C. Of greater significance, is that the crossover point has again shifted by RFEM as it seeks out the weakest path through the slope. In Figure 20, the crossover occurs at $FS \approx 1.37$ which is significantly higher and of greater practical significance than the crossover point of $FS \approx 1.12$ by finite element local averaging alone. The theoretical line corresponding to $\Theta_C = \infty$ is also shown in this plot. From a practical viewpoint, the RFEM analysis indicates that failure to properly account for local averaging is unconservative over a wider range of Factors of Safety than would be the case by finite element local averaging alone. To further highlight this difference, the particular results from Figures 19 and 20 corresponding to $\Theta_C = 0.5$ (spatial correlation length equal to half the embankment height) have been re plotted in Figure 21.

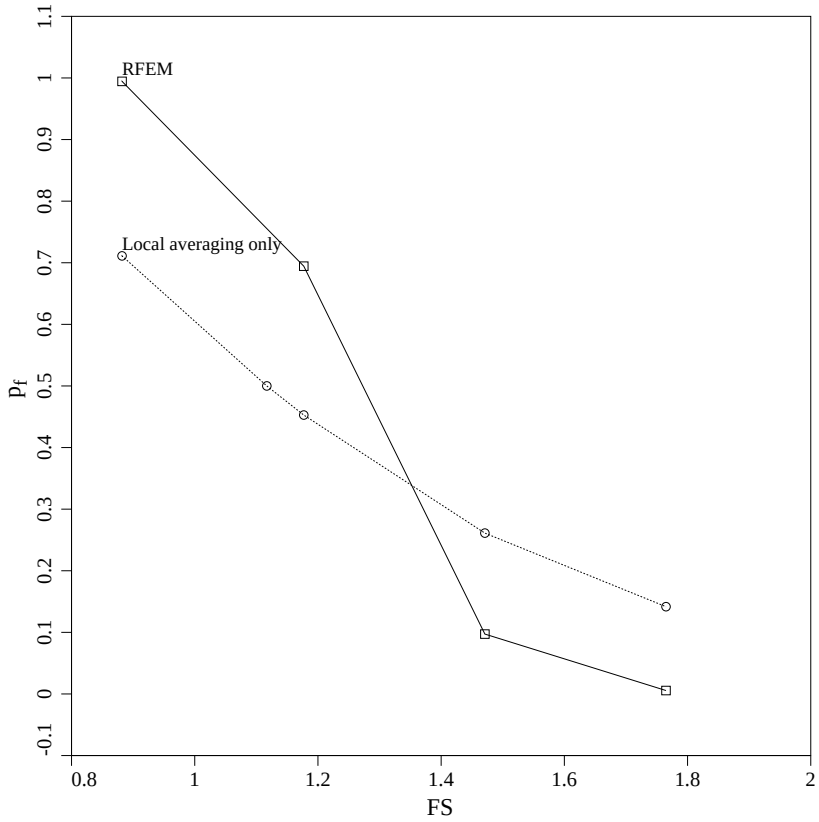

Figure 21. Probability of Failure vs. Factor of Safety (based on the mean) using finite element local averaging alone and RFEM for the test slope. $V_C = 0.5$ and Θ_C=0.5

11 Concluding remarks

The paper has investigated the probability of failure of a cohesive slope using both simple and more advanced probabilistic analysis tools. The simple approach treated the strength of the entire slope as a single random variable, ignoring spatial correlation and local averaging. In the simple studies, the Probability of Failure was estimated as the probability that the shear strength would fall below a critical value based on a lognormal probability density function. These results led to a discussion on the appropriate choice of a design shear strength value suitable for deterministic analysis. Two factorization methods were proposed that were able to bring the Probability of Failure and the Factor of Safety more into line with practical experience.

The second half of the paper implemented the random finite element method (RFEM) on the same test problem. The non-linear elasto-plastic analyses with Monte-Carlo simulation were able to take full account of spatial correlation and local averaging, and observe their impact on the Probability of Failure using a parametric approach. The elasto-plastic finite element slope stability method makes no *a priori* assumptions about the shape or location of the critical failure mechanism, and therefore offers very significant benefits over traditional limit equilibrium methods in the analysis of highly variable soils. In the elasto-plastic RFEM, the failure mechanism is free to "seek out" the weakest path through the soil and it has been shown that this generality can lead to higher probabilities of failure than could be explained by finite element local averaging alone.

In summary, simplified probabilistic analysis, in which spatial variability is ignored by assuming perfect correlation, can lead to unconservative estimates of the probability of failure. This effect is most pronounced at relatively low factors of safety (Figure 20) or when the coefficient of variation of the soil strength is relatively high (Figure 18).

12 Acknowledgment

The writers wish to acknowledge the support of NSF Grant No. CMS-9877189.

13 Notation

c_u	Undrained shear strength
C	Dimensionless shear strength
C_{des}	Design value of C
D	Foundation depth ratio
f_1	Linear strength reduction factor
f_2	Strength reduction factor based on standard deviation
FS	Factor of Safety
H	Height of slope
p_f	Probability of Failure
V_C	Coefficient of variation of C
x	Cartesian x-coordinate
y	Cartesian y-coordinate
α	Dimensionless element size parameter
β	Slope angle
γ	Variance reduction factor
γ_{sat}	Saturated unit weight
θ_C	Spatial correlation length of C
$\theta_{\ln C}$	Spatial correlation length of $\ln C$
Θ_C	Dimensionless spatial correlation length of $\ln C$
μ_C	Mean of C
$\mu_{\ln C}$	Mean of $\ln C$
$\mu_{\ln C_A}$	Locally averaged mean of $\ln C$ over a square finite element
μ_{C_A}	Locally averaged mean of C over a square finite element
ρ	Correlation coefficient
σ_C	Standard deviation of C
σ_{C_A}	Locally averaged standard deviation of C over a square finite element
$\sigma_{\ln C}$	Standard deviation of $\ln C$
$\sigma_{\ln C_A}$	Locally averaged standard deviation of $\ln C$ over a square finite element
τ	Absolute distance between two points
τ_x	x-component of distance between two points
τ_y	y-component of distance between two points
ϕ_u	Undrained friction angle

Bibliography

E.E. Alonso. Risk analysis of slopes and its application to slopes in Canadian sensitive clays. *Géotechnique*, 26(453-472), 1976.

A.W. Bishop. The use of the slip circle in the stability analysis of slopes. *Géotechnique*, 5(1):7–17, 1955.

R.N. Chowdhury and W.H. Tang. Comparison of risk models for slopes. In *Proceedings*

of the Fifth International Conference on Applications of Statistics and Probability in Soil and Structural Engineering, volume 2, pages 863–869. Vancouver, B.C., 1987.

J.T. Christian. Reliability methods for stability of existing slopes. In C.D. Shackelford *et al*, editor, *Uncertainty in the geologic environment: From theory to practice*, pages 409–419. GSP 58, ASCE, 1996. Wisconsin, August 1996.

J.T. Christian, C.C. Ladd, and G.B. Baecher. Reliability appled to slope stability analysis. *J Geotech Eng, ASCE*, 120(12):2180–2207, 1994.

R. A. D'Andrea and D. A. Sangrey. Safety factors for probabilistic slope design. *J Geotech Eng, ASCE*, 108(9):1108–1118, 1982.

J. M. Duncan. Factors of safety and reliability in geotechnical engineering. *J Geotech Geoenv Eng, ASCE*, 126(4):307–316, 2000.

H. El-Ramly, N.R. Morgenstern, and D.M. Cruden. Probabilistic slope stability analysis for practice. *Can Geotech J*, 39:665–683, 2002.

G. A. Fenton and D. V. Griffiths. Statistics of flow through a simple bounded stochastic medium. *Water Resour Res*, 29(6):1825–1830, 1993.

G.A. Fenton and E.H. Vanmarcke. Simulation of random fields via local average subdivision. *J Eng Mech, ASCE*, 116(8):1733–1749, 1990.

D. V. Griffiths and G. A. Fenton. Bearing capacity of spatially random soil: the undrained clay Prandtl problem revisited. *Géotechnique*, 51(4):351–359, 2001.

D. V. Griffiths and G. A. Fenton. Influence of soil strength spatial variability on the stability of an undrained clay slope by finite elements. In *Slope Stability 2000, Proceeding of GeoDenver 2000*, pages 184–193. ASCE, 2000.

D. V. Griffiths and P. A. Lane. Slope stability analysis by finite elements. *Géotechnique*, 49(3):387–403, 1999.

A.M. Hassan and T.F. Wolff. Effect of deterministic and probabilistic models on slope reliability index. In D. V. Griffiths *et al*, editor, *Slope Stability 2000*, pages 194–208. ASCE, 2000. GSP No. 101.

F.H. Kulhawy, M.J.S. Roth, and M.D. Grigoriu. Some statistical evaluations of geotechnical properties. In *Proc. ICASP6, 6th Int. Conf. Appl. Stats. Prob. Civ. Eng.* 1991.

S. Lacasse. Reliability and probabilistic methods. In *Proc 13th Int Conf Soil Mech Found Eng*, pages 225–227. 1994. New Delhi, India.

S. Lacasse and F. Nadim. Uncertainties in characterising soil properties. In C.D. Shackelford *et al*, editor, *Geotechnical Special Publication No 58, Proceedings of Uncertainity '96 held in Madison, Wisconson, July 31 - August 3, 1996*, pages 49–75. GSP 58, ASCE, 1996.

I. K. Lee, W. White, and O. G. Ingles. *Geotechnical Engineering*. Pitman, London, 1983.

K.S. Li and P. Lumb. Probabilistic design of slopes. *Can Geotech J*, 24:520–531, 1987.

M. Matsuo and K. Kuroda. Probabilistic approach to the design of embankments. *Soils Found*, 14(1):1–17, 1974.

G.R. Mostyn and K.S. Li. Probabilistic slope stability – State of play. In K.S. Li and S-C.R. Lo, editors, *Proc. Conf. Probabilistic Meths. Geotech. Eng.*, pages 89–110. A. A. Balkema, Rotterdam, 1993.

G.R. Mostyn and S. Soo. The effect of autocorrelation on the probability of failure of slopes. In *6th Australia, New Zealand Conference on Geomechanics: Geotechnical Risk*, pages 542–546. 1992.

G.M. Paice. *Finite element analysis of stochastic soils*. PhD thesis, University of Manchester, U.K., 1997.

I. M. Smith and D. V. Griffiths. *Programming the Finite Element Method*. John Wiley and Sons, Chichester, New York, 3rd edition, 1998.

W.H. Tang, M.S. Yucemen, and A.H.S. Ang. Probability based short-term design of slopes. *Can Geotech J*, 13:201–215, 1976.

D. W. Taylor. Stability of earth slopes. *J. Boston Soc. Civ. Eng.*, 24:197–246, 1937.

E.H. Vanmarcke. *Random fields: Analysis and synthesis*. The MIT Press, Cambridge, Mass., 1984.

E.H. Vanmarcke. Reliability of earth slopes. *J Geotech Eng, ASCE*, 103(11):1247–1265, 1977.

R.V. Whitman. Organizing and evaluating in geotechnical engineering. *J Geotech Geoenv Eng, ASCE*, 126(7):583–593, 2000.

T.F. Wolff. Probabilistic slope stability in theory and practice. In C.D. Shackelford *et al*, editor, *Uncertainty in the geologic environment: From theory to practice*, pages 419–433. GSP 58, ASCE, 1996. Wisconsin, August 1996.